Supplementary Information

The Cryo-EM structure of human CD163 bound to haptoglobin-hemoglobin reveals molecular mechanisms of hemoglobin scavenging.

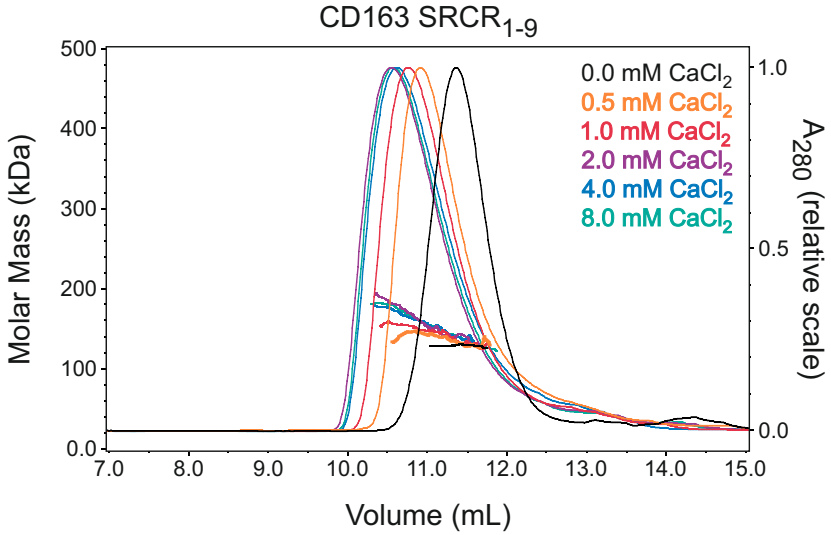

Supplementary Figure 1. Calcium dependence of CD163 oligomerization. SEC-MALS analysis of CD163 SRCR 1-9 in the presence of varying $CaCl_2$ concentrations. The measured molecular weights of the chromatogram peaks are shown as thick lines. This experiment used a 24 ml Superdex 200 Increase 10/300 GL column, in contrast to the 15 ml Wyatt SEC Analytical Column (WTC-030S5) used in the experiments shown in Figure 1. The larger sample dilution on the Superdex 200 Increase 10/300 GL column results in a slightly lower measurement of the sample mass likely due to complex dissociation.

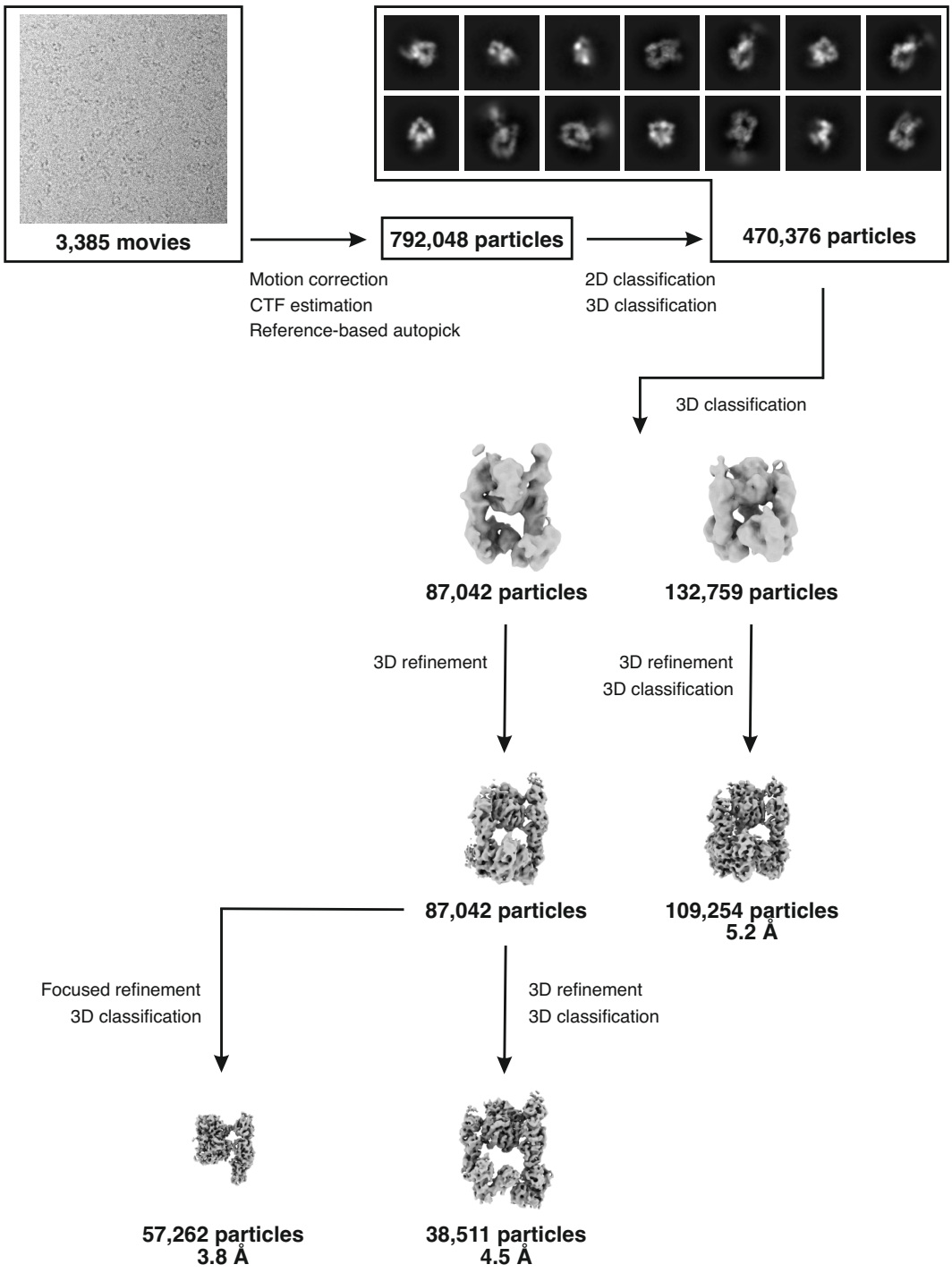

Supplementary Figure 2. Cryo-EM data particle processing workflow. Single particle analysis scheme for the CD1631-9-HpHb complex.

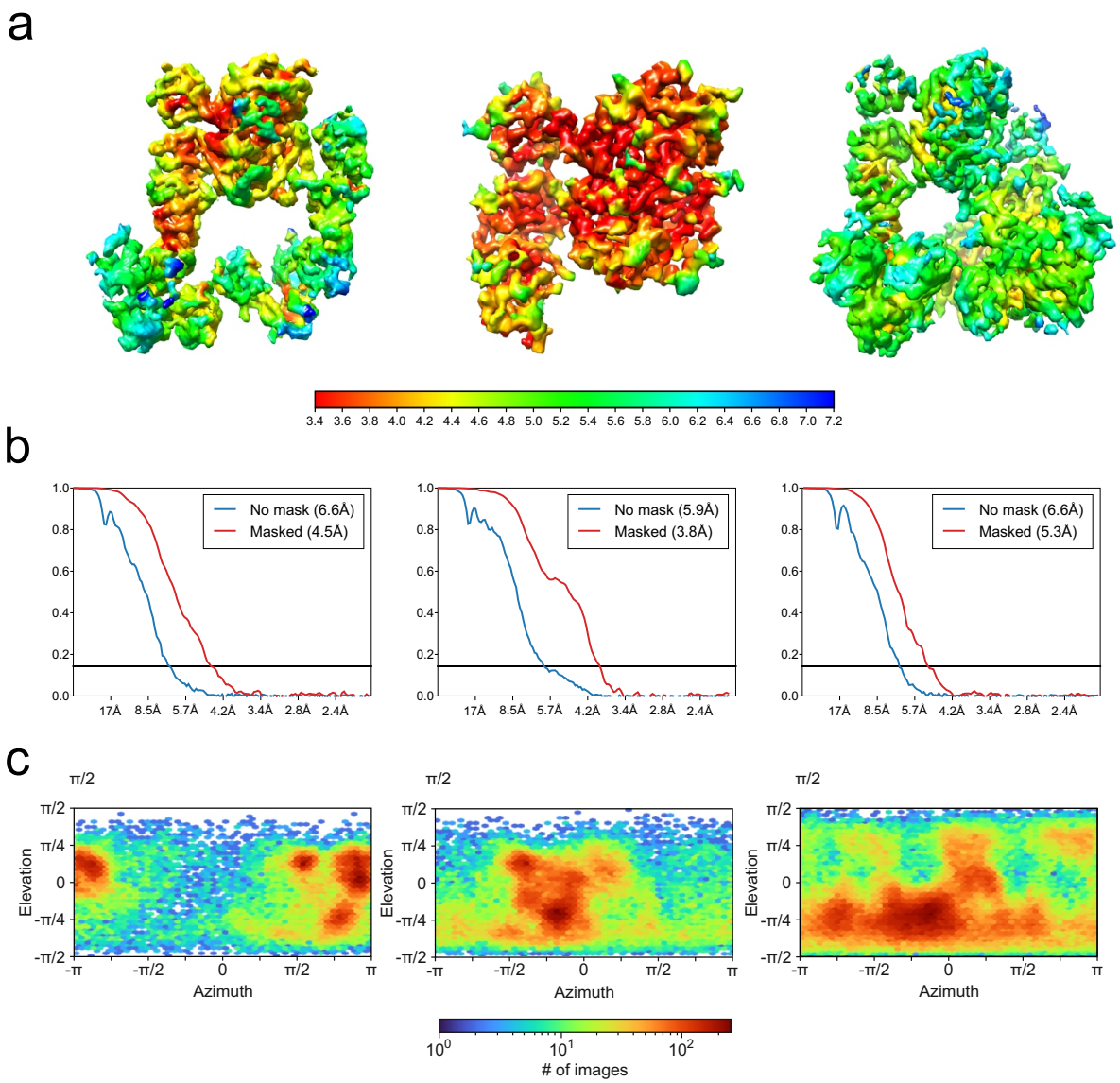

Supplementary Figure 3. Local resolution maps of CD163-HpHb and Fourier shell correlation curves. **a**. Local resolution maps of the cryo-EM maps presented in Figure 1. Left: CryoEM density map of dimeric CD163 SRCR 1-9 bound to HpHb (4.5 Å resolution), middle: CryoEM density map from focused refinement using a mask covering CD163-A SRCR 2-4 and HpHb (3.8 Å resolution), Right: CryoEM density map of trimeric CD163 SRCR 1-9 bound to HpHb (5.3 Å resolution). **b**. Fourier shell correlation curves of the maps shown in a. **c.** Viewing direction distribution of the maps shown in a.

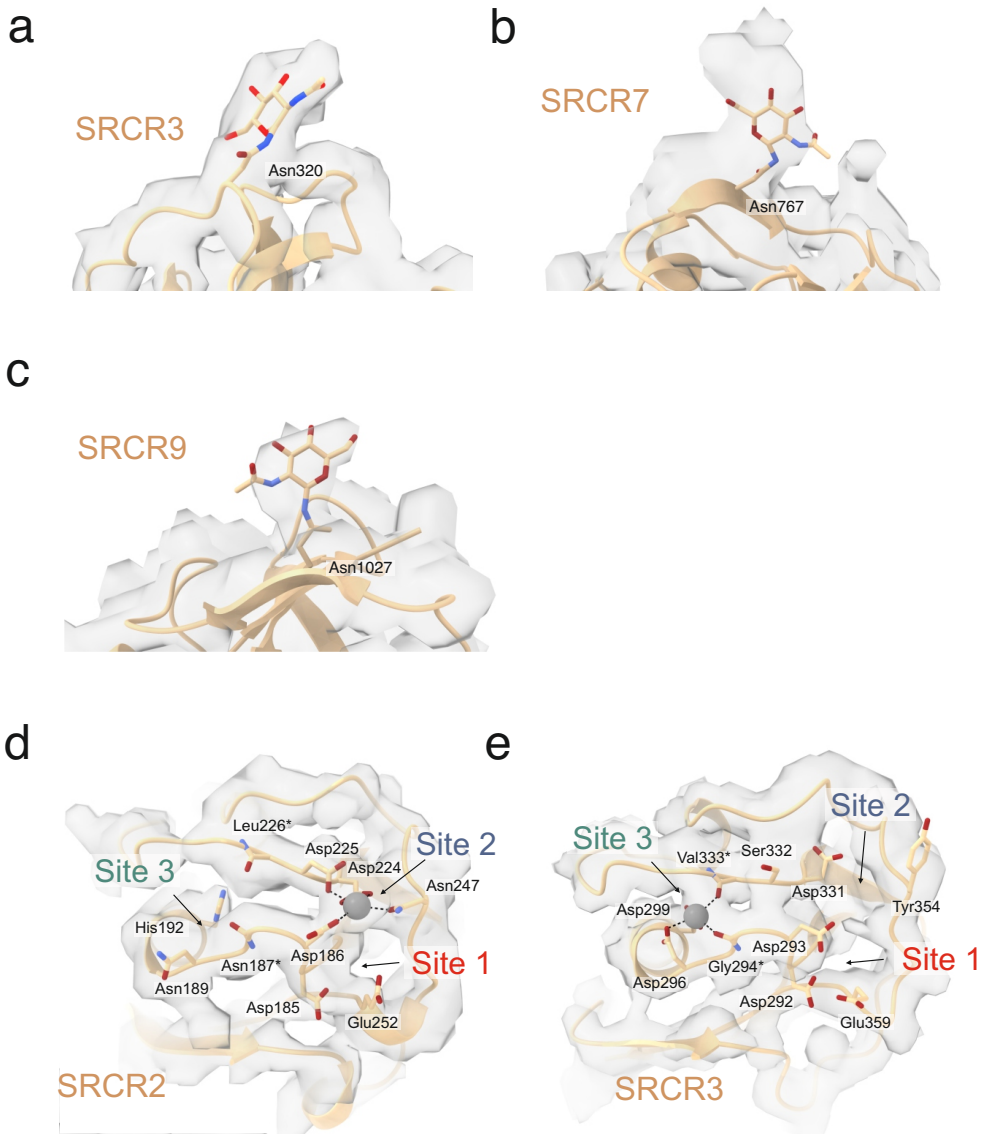

Supplementary Figure 4. Cryp-EM densities of N-linked glycosylations and Ca^{2+} ions. a-c. Density maps of $CD163_A$ SRCR3 (a), SRCR7 (b) and SRCR9 (c). Asparagine residues and N-acetylgalactosamines are shown as sticks. **d+e**. Density maps of $CD163_A$ SRCR2 (d) and $CD163_A$ SRCR3 (e). Residues constituting the three canonical Ca^{2+}-binding sites are shown as sticks.

Supplementary Figure 5

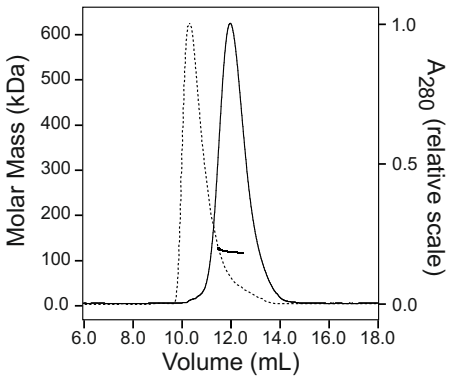

Supplementary Figure 5. Oligomerization of CD163 1-9 D745A/D746A/D955A/D956A. SEC-MALS analysis of CD163 SRCR 1-9 **D745A/D746A/D955A/D956A**. The measured molecular weights of the chromatogram peaks are shown as thick lines. A chromatogram of wild-type CD163 SRCR 1-9 is shown with dashes for comparison.

Supplementary Figure 6

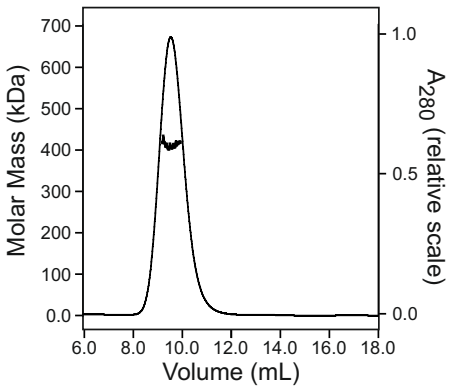

Supplementary Figure 6. Trimerization of CD163-CC. SEC-MALS analysis of CD163-CC is shown, with the measured molecular weight of the chromatogram peak represented by a thick line. The monodisperse peak in the chromatogram confirms that CD163-CC forms an intact trimer, with a measured molecular weight of approximately 410 kDa, closely matching the expected weight of 420 kDa.

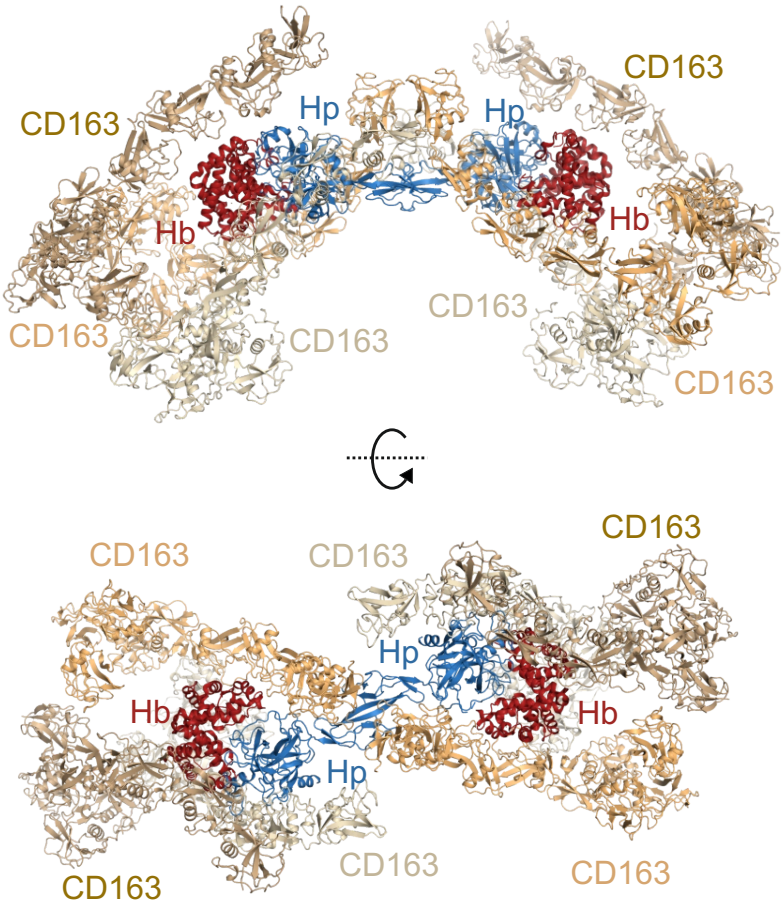

Supplementary Figure 7. Model of CD163 Trimers Bound to Dimeric Hp(1-1)Hb.

Cartoon representation of a model of CD163 trimers (orange) bound to both ends of the dimeric Hp(1-1)Hb complex (blue/red). The bottom figure is rotated 90 degrees relative to the top view. The position of CD163 SRCR1 was modeled based on the AlphaFold2 structural prediction of CD163.

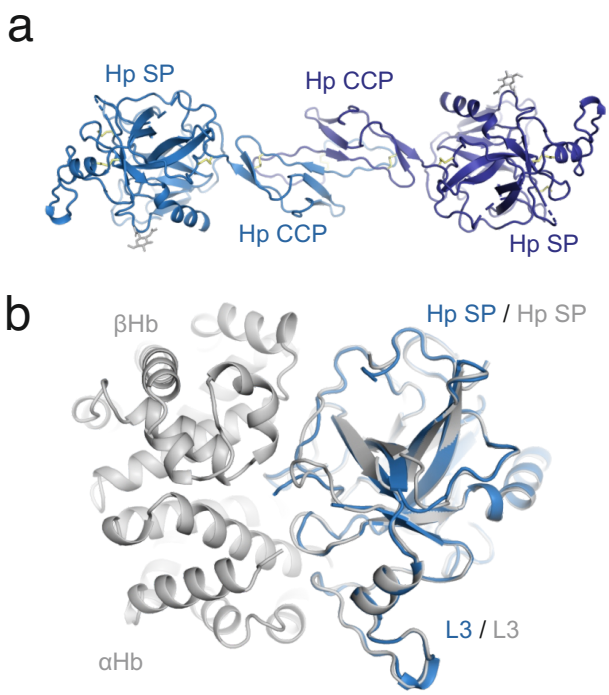

Supplementary Figure 8. Structure of human Hp. a. Cartoon representation of the crystal structure of dimeric human Hp(1-1). The two subunits are colored light blue and dark blue, respectively. Disulfide bridges are shown as yellow sticks and N-linked glycosylations as grey sticks. **b**. Superimposition of Hp (light blue) and αβHb-bound Hp (grey).

	$CD163_2$-HpHb (EMDB-50444) (PDB 9FHB)	$CD163_2$-HpHb (EMDB-50570) (PDB 9FMU)	$CD163_3$-HpHb (EMDB-50600) (PDB 9FNO)
Data collection and processing			
Detector	Gatan K2 summit	Gatan K2 summit	Gatan K2 summit
Voltage (kV)	300	300	300
Electron exposure (e–/Å^2)	90	90	90
Defocus range (μm)	500-1500	500-1500	500-1500
Pixel size (Å)	1.06	1.06	1.06
Initial particle images (no.)	792,048	792,048	792,048
Final particle images (no.)	57,262	32,511	109,254
Map resolution (Å)	3.87	4.46	5.20
FSC threshold	0.143	0.143	0.143
Refinement			
Model composition			
Non-hydrogen atoms	6755		
Protein residues	6625		
Ligands	130		
R.m.s. deviations			
Bond lengths (Å)	0.005		
Bond angles (°)	0.951		
Validation			
MolProbity score	2.41		
Clashscore	16.23		
Poor rotamers (%)	2.82		
Ramachandran plot			
Favored (%)	95.07		
Allowed (%)	4.11		
Disallowed (%)	0.82		

Supplementary Table 1. Cryo-EM data collection, refinement and validation statistics.

SRCR structure in the Protein Data Bank				Crystallization conditions	
ID	Name	Site occupancy	Sequence (site1,site2,site3)	Ca^{2+}	Mg^{2+}
8J8T	hDMBT1 SRCR11	① ② ③	VCDDYWDTNDA VLDDVRC HNCG---HHEDAGVICS	200 mM	0 mM
6SAN	hDMBT1 SRCR8	① ② ③	VCDDSWDTNDA VLDDVRC HNCG---HSEDAGVICS	10 mM	10 mM
7DPX	hSCARA1 SRCR	①	ICDDRWEVRVG WLNEVFC RACS---HSEDAGVTCT	2 mM	0 mM
6J02	mSCARA1 SRCR	①	ICDDRWDIRAG WLNEVMC LSCS---HSEDAGVTCT	10 mM	0 mM
7C00	hSCARA5 SRCR	① ② ③	VCDDGWDKKDG WMDDVAC TNCG---HAEDASVTCN	1.5 mM	0 mM
7BZZ	mSCARA5 SRCR	① ② ③	VCDDGWDKKDG WMDDVNC TNCG---HAEDAGVTCT	1.5 mM	0 mM
6SA4	hDMBT1 SRCR1	1 2 ③	VCDDSWDTNDA ALDDVRC HNCG---HGEDAGVICS	0 mM	200 mM
6SA5	hDMBT1 SRCR8	1 2 ③	VCDDSWDTNDA VLDDVRC HNCG---HSEDAGVICS	0 mM	200 mM
2OY3	MARCO SRCR	① 3	ICDDDWDNNDA WLDNVNC HNCV---HNEDAGVECS	0 mM	0 mM*
8J8D	hDMBT1 SRCR11	1 2 3	VCDDYWDTNDA VLDDVRC HNCG---HHEDAGVICS	N/A	N/A
8H7J	pCD163 SRCR5		VCDSDFSLEAA WAEEFQC GTCS---HSRDVGVVCS	N/A	N/A
8H7J	pCD163 SRCR6	3	LCNSHWDMEDA WRHMFHC SLCS---SGQVASVICS	N/A	N/A
8H7J	pCD163 SRCR7	1 3	ICDDSWDLNDA WLDEINC HNCR---HKEDAGVICS	N/A	N/A
8H7J	pCD163 SRCR8		VGRNSMSPATV WVDNVQC RLAS---PSEETWITCA	N/A	N/A
8H7J	pCD163 SRCR9	1 3	VCDDSWDLEDA WLNEVKC SDCG---HKEDAAVTCS	N/A	N/A
6K0L	sCD163 SRCR5		VCDSDFSLEAA WTEEFQC GTCS---HSRDVGVVCS	0 mM	0 mM
6K0O	CD163L1 SRCR8		VCDSDFSLHAA WAEKFQC DTCI---HSREVGVVCS	0 mM	0 mM
5HRJ	pCD163 SRCR5		VCDSDFSLEAA WAEEFQC GTCS---HSRDVGVVCS	0 mM	0 mM
5JFB	pCD163 SRCR5		VCDSDFSLEAA WAEEFQC GTCS---HSRDVGVVCS	0 mM	0 mM
6H8M	Neurotrypsin	1	ICDDGWTDKHA HMDNVKC HNCR---HSEDAGVICD	0 mM	0 mM
5A2E	CD6 SRCR1		ACGALWDSRAA GAPALLC HACRS—DGRRARVTCA	0 mM	0 mM
5A2E	CD6 SRCR2	1 3	VCDDTWDLEDA HRDQVNC HYCG---HKEDAGAVCS	0 mM	0 mM
5A2E	CD6 SRCR3		VCDSEWYPSEA -RMYYSC NLCS---QSLAARVLCS	0 mM	0 mM
5ZE3	LOXL2 SRCR3	1	VCDDKWDLVSA HLNEIQC QGCN---HEEDAGVRCN	0 mM	0 mM
5ZE3	LOXL2 SRCR4		VCGQNWGIVEA VMSGVKC VACPQGGVQYGAGVACS	0 mM	0 mM
2OYA	MARCO SRCR	1 3	ICDDDWDNNDA WLDNVNC HNCV---HNEDAGVECS	0 mM	0 mM
1BY2	Gal3bp SRCR	3	VCDNLWDLTDA MLDEVQC SNCR---HERDAGVVCT	0 mM	0 mM

Supplementary Table 2. Overview of SRCR structures and Ca^{2+}-site occupancy. Table of SRCR structures in the protein data bank. In column 3, numbered grey spheres represent occupied Ca^{2+}-binding sites and numbers represent unoccupied intact canonical sites. (*) The crystals may contain traces of Mg^{2+} from purification. The content of the crystallization buffer in not available for unpublished structures (N/A).

	hHp
Data collection	
Space group	C2
Cell dimensions	
a, *b*, *c* (Å)	89.9, 77.7, 65.1
α, β, γ (°)	90.0, 92.5, 90.0
Wavelength	1.038
Resolution (Å)	50-2.5 (2.6-2.5)
R_{sym}	0.047 (0.218)
$I / \sigma I$	20.23 (5.45)
Completeness (%)	95.6 (67.2)
Redundancy	4.18 (3.18)
Refinement	
Resolution (Å)	2.5
No. reflections	14717
R_{work} / R_{free}	0.191 / 0.227
No. atoms	
Protein	2451
Carbohydrate	14
Water	93
B-factors	
Protein	53.7
Carbohydrate	73.0
Water	54.1
R.m.s deviations	
Bond lengths (Å)	0.002
Bond angles (°)	0.585

Supplementary Table 3. Data collection, phasing and refinement statistics. Values in parentheses are for highest-resolution shell.